www.czasopisma.pan.pl PAN www.journals.pan.pl

ARCHIVES of FOUNDRY ENGINEERING

VERSITA

DOI: 10.2478/v10266-012-0061-6

Published quarterly as the organ of the Foundry Commission of the Polish Academy of Sciences

ISSN (2299-2944)
Volume 12
Issue 2/2012

187 – 204

Effect of Annealing Time for Quenching CuAl7Fe5Ni5W2Si2 Bronze on the Microstructure and Mechanical Properties

B. P. Pisarek*
Department of Materials Engineering and Production Systems, Technical University of Lodz
1/15 Stefanowskiego Street 90-924 Lodz, Poland
*Corresponding author. E-mail address: boguslaw.pisarek@p.lodz.pl

Received 25-05-2012; accepted in revised form 31-05-2012

Abstract

This paper presents the influence of annealing time 30, 60 and 120 min at 1000°C for quenching CuAl7Fe5Ni5W2Si2 bronze in 10% water solution of NaCl, on the microstructure and mechanical properties. The presented results concern the species newly developed aluminum-iron-nickel bronze, with additions W and Si.

In order to determine changes in the microstructure of the hardened bronze metallographic studies were performed on cylindrical samples of diameter 10 mm, on the metallographic microscope with digital image analysis, X-ray phase analysis, EDX point with the digital recording on the computer. Specified percentage of the microstructure of martensite and bainite, participation of proeutectoid α phase in the microstructure, grain size of former β phase, the amount of dissolved κ phase.

It was found that in the microstructure of bronze in the cast state, there are a number of intermetallic phases of κ type. At interphase boundaries of primary intermetallic faceted precipitates, especially rich in tungsten (IM_W), nucleate and grow dendritic primary intermetallic κ_I phases, with chemical composition similar to the type of Fe_3Si iron silicide.

Dissolved, during the heating, in the β phase are all the intermediate phase included in the microstructure, with the exception of primary intermetallic phases of tungsten and κ_I. Prolongation of the isothermal annealing causes coagulation and coalescence of primary phases. In microstructure of the bronze after quenching obtained the α phase precipitation on the grain boundary of secondary β phase, coarse bainite and martensite, for all annealing times. With the change of annealing time are changed the relative proportions of individual phases or their systems, in the microstructure. In the microstructure of bronze, hold at temperature of 1000°C for 60 min, after quenching martensitic microstructure was obtained with the primary phases, and the least amount of bainite.

Keywords: Innovative Foundry Technologies and Materials, Annealing, Quenching, Microstructure, Mechanical Properties, Al-Fe-Ni-W-Si Bronze

1. Introduction and purpose

The presented in Figure 1, the equilibrium phase diagram of Cu-Al-5% Fe-5% Ni shows that the microstructure of aluminum bronze with the addition of Fe and Ni (in the amount of 5% each), only one κ phase crystallizes [1]. As a result of the relatively low solubility of additives elements input (except Ni) in the basic phases of aluminum bronze metallic matrix, formed during the

crystallization of α and β phases are characterized by large dendritic microsegregation.

An analysis of the current state of knowledge indicates that the microstructure hypoeutectoid aluminum bronze with additions of Fe, Ni, Si and Mn, at ambient temperature, may be present a lot of hard intermetallic phases of κ type [1÷3]. Characteristic of these phases is that they contain except to Ni, elements with low solubility in solutions of β and α, characteristic for the matrix aluminum bronze. Table 1 shows the types of κ phase identified in the aluminum bronzes and concentration of their constituent elements. It is possible to distinguish two groups generally, the first group is rich intermetallic phases mainly Fe (κ_{Fe}, κ_I, κ_{II} and κ_{IV}) and the second group phase, especially rich in Ni (κ_{Ni}, κ_{III}). Depending on the type of elements and their amounts in aluminum bronze can also crystallize intermetallic phases of type: FeAl, Fe_3Al, $(Fe,Cu)_3Al$ and NiAl, Ni_3Al.

Analyzing the phase equilibrium diagram (Fig. 1) and the resulting microstructure of bronze with different number of elements input in amounts of alloying to aluminum bronzes, the formation of the microstructure takes place as follows. In the hypoeutectoid aluminum bronzes with increased concentrations of Fe, Ni and/or Si [1÷3], or Cr, Mo, W [4÷9] can nucleate and grow primary κ_I intermetallic phase. It crystallizes at a higher temperature than the β phase, growing dendritically from the liquid alloy. When crystallized κ_I phase nucleates and grows with the rest of the liquid alloy β phase.

After overcooling the equilibrium solvus temperature nucleates and grows intermetallic phase κ_{II} at phase boundary and inside the β phase. Crystallization of this phase included only the equilibrium phase diagram of Cu-Al-5% Fe-5% Ni by marking it "κ" (Fig. 1).

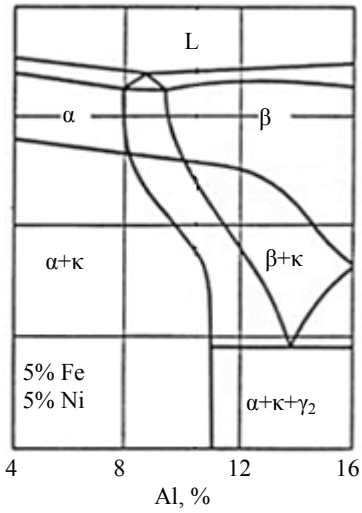

Fig. 1. Vertical section through Cu-Al-5%Ni-5%Fe phase diagram [1]

After the bronze overcooling below the solvus temperature further, by increasing the solubility of Al in β phase, followed by diffusion of Al into the β phase and dealuminization β phase transforms into the α phase. This transformation begins from the β phase boundaries, and includes the interior in places poorer in Al. During this partial transformation of β phase in α phase, probably due to the decreasing solubility of Fe and Ni additives in the α phase with decreasing temperature, in the newly formed α phase, intermetallic phases are formed κ_{III} and κ_{IV}. Phase κ_{III} isolated in the form of tiles in the areas of α phase richer in Ni, and phase κ_{IV} in the areas of α phase richer in Fe.

Because of the higher melting point of Fe (1535°C) of Ni (1455°C), probably at a higher temperature κ_{IV} phase is precipitated rich in iron, and the lower κ_{III} phase rich in nickel. This does not exclude the possibility that the α phase precipitation processes of intermetallic κ_{III} and κ_{IV} phases occur at the same temperature range, but include other areas of the α phase.

Table 1.
The chemical composition of κ-type intermetallic phases crystallizing in aluminum-iron-nickel bronze

Phase	Chemical composition, %						References
	Al	Fe	Ni	Cu	Si	Mn	
κ_{Fe}	19.8	50.9	15.0	14.3	-	-	[2]
κ_I	13.0±5.0	55.0± 7.0	15.0±3.0	15.0±5.0	-	2.0±0.4	[10]
	10.0±1.3	72.0±14.0	3.5±4.0	9.5	1.6±0.4	2.9±0.5	[11]
κ_{II}	19.0	32.0± 3.0	27.0±5.0	19.0	-	2.0	[10]
	12.3±1.3	61.3± 4.9	8.0±1.8	12.1±3.0	4.1±0.8	2.0±0.4	[11]
κ_{IV}	15.0±5.0	62.0± 6.0	10.0±5.0	14.0±5.0	-	1.3±0.4	[10]
	10.5±1.7	73.0± 2.0	7.3±1.5	26.0±7.0	4.0±1.5	2.4±0.2	[11]
κ_{Ni}	19.1	25.8	40.1	15.0	-	-	[2]
κ_{III}	20.0±4.0	30.0± 3.0	32.0±2.0	26.0±4.0	-	1.8±0.4	[10]
	26.7±1.0	12.8± 1.6	41.3±6.0	17.0±5.0	<0.1	2.0±0.4	[11]

After the bronze overcooling below the equilibrium eutectoid transformation temperature of the remaining β phase rich in Al, is formed eutectoid $\alpha + \gamma_2$.

Due to the presence in the microstructure of complex aluminum bronzes in the cast state, a series of hard phases κ (κ_I, κ_{II}, κ_{III}, κ_{IV}), the heat treatment process it is possible to carry out the treatments involving the precipitation strengthening of the bronze matrix hyperquenching and aging process, as well as the formation of martensite and/or bainite from saturated of admixtures β phase and new κ phase (κ_V) [3,4].

In Figure 2 (a, b) are shown values of the coefficient of thermal conductivity λ W/m•K and heat capacity Cp, J/kg•K for typical aluminum bronze elements (a), the coefficient of λ and heat capacity Cp for copper and bronze casting (b) [13,14]. Make additions aluminium bronze admixtures significantly reduce the alloy conductivity coefficient λ, compared to the coefficient of λ for the copper and have a significant effect on the heat capacity Cp, which in turn strongly influences the cooling rate during intense cooling of the alloy.

a)

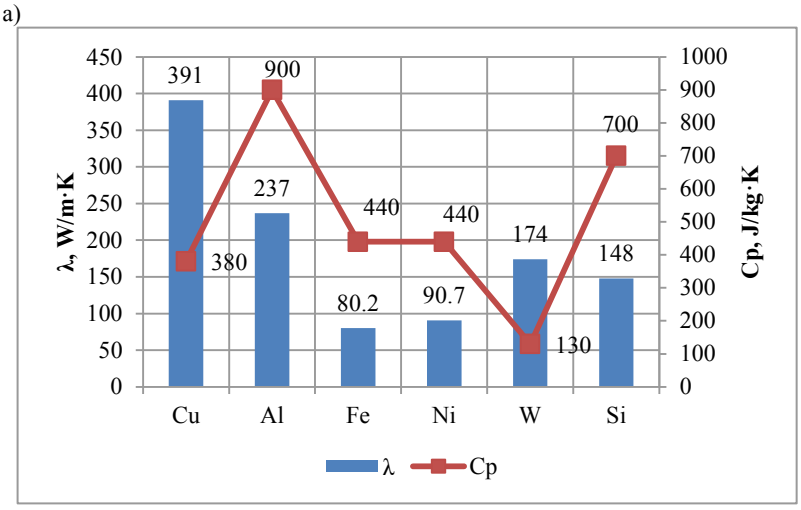

b)

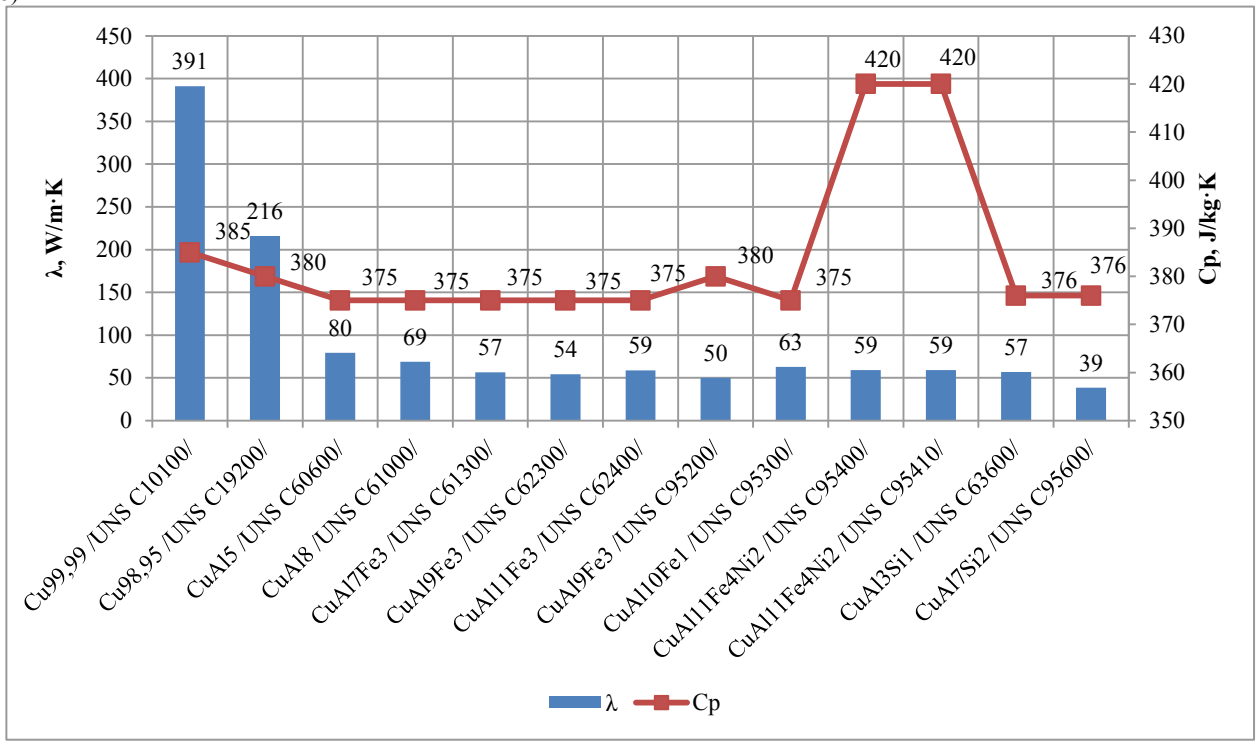

Fig. 2. Thermal conductivity λ and heat capacity Cp of the elements (a) [13] and copper and its alloys (b) [14]

The aim of this study was to investigate the effect of annealing time CuAl7Fe5Ni5W2Si2 bronze, tempered with 10% NaCl solution in water, the change: the percentage of the microstructure of martensite and bainite, proeutectoid α phase, grain size (area and length of the intergranular boundary) of the former β phase, the number of dissolved phase κ.

The study arose from studies in the Department of Materials Engineering and Production Systems TUL new grades of aluminum-iron-nickel bronze, with additions individually or simultaneously Cr, Mo, W, Si and/or C [4÷9,15,16]. Knowledge of the effect of heat treatment parameters such as temperature and holding time to the process of quenching on the microstructure of newly developed bronzes can control their properties in the casting.

2. Description of research

2.1. Research methodology

CuAl7Ni5Fe5W2Si2 bronze melted in a laboratory induction furnace crucible a capacity of 15 kg and frequency of 8 kHz. Each time charcoal was spread on the metallic charge, with the task of limiting access of oxygen to the liquid alloy. Alloy was withstand in a temperature of 1300°C ± 15°C. The slag covering and refining UNITOP BA-1 was dosed as follows: half of the slag was added to the so-called cold metallic charge, and the rest after melting the charge. After melting bronze and isothermal heating slag removed and refined N_2 for 5 min. Then added 0.6% of the mass of metal charge modifier Aluminum-Beryllium 5%, waited 3 minutes and pouring sand mold. Sample castings were made in molds from wet molding sand.

In Figure 3 (a, b) are shown the dimensions measuring sample (after machining) to test its temperature during heat treatment (a) and measuring position (b).

The theoretical temperature of the sample during heat treatment and heat treatment of the characteristic parameters of the tested bronze samples shown in Figure 4. The heat treatment process consisted of the following steps: T1 - heating, T2 - annealing at 1000°C, T3 - cooling in ambient air (sample temperature ≥950°C) at the time necessary to remove the sample from the oven and T4 - immersion in a tank with 10% NaCl in water at 19°C (hyperquenching and hardening). During all stages of heat treatment temperature of the sample was measured thermocouple Pt-PtRh10 using Crystaldigraph devices and recorded in computer memory.

After heat treatment of the sample (Fig. 3a), with a section of solid section, cut off roller 10 mm in length (measured from the front of the sample). The roller was a sample for further metallographic examination. Metallographic specimen made on the surface of roller cut from measuring sample.

Microstructure of bronze identified at the metallographic microscope on metallographic specimen etched Mi15Cu reagent. Using a computer program for digital image analysis MultiScanBase, determined the percentage of martensite and bainite microstructure, participation in the proeutectoid α phase microstructure, grain size (area and length of the interface) of the former β phase, the amount of dissolved κ phase.

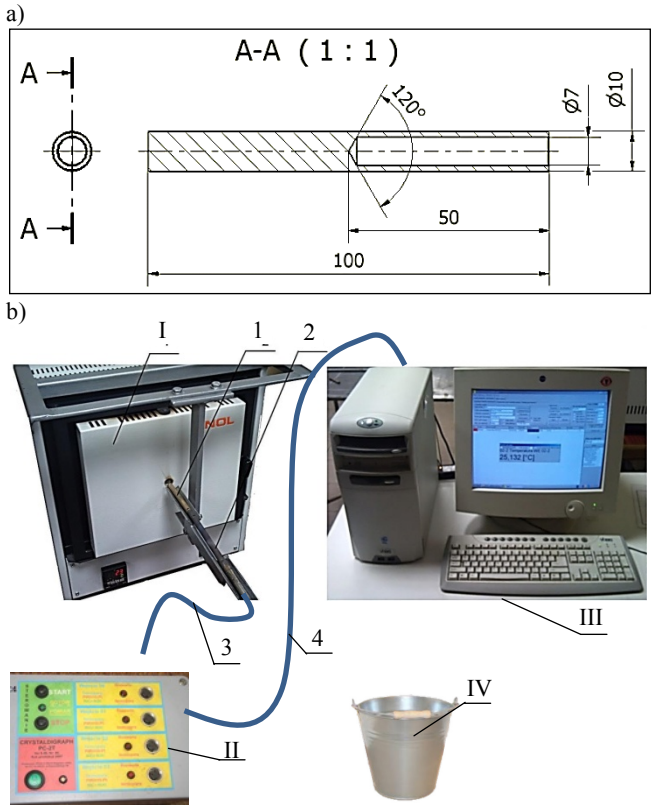

Fig. 3. The dimensions of the sample (a) and position measurement (b): I - resistance furnace, II - Crystaldigraph, III - computer; IV - receptacle with 10% NaCl in water, 1 - sample from the study bronze, 2 - lance with thermocouple Pt-PtRh10, 3 - compensating lead, 4 - line transmission

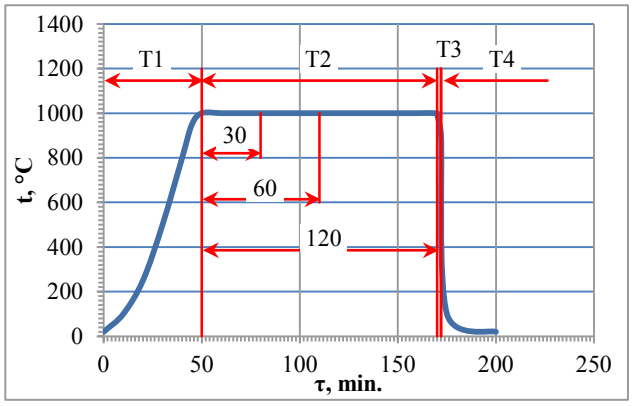

Fig. 4. The theoretical temperature of the sample during heat treatment and heat treatment program: T1 - heating, T2 - annealing, T3 - cooling in ambient air, T4 - cooling in 10% NaCl solution in water, 30, 60, 120: a sample annealing time in minutes

X-ray phase analysis was carried out on a JEOL JDX-7S diffractometer using a lamp with copper anode (CuK – 1.5406 Å)

at a supply current of 20 mA at 40 kV, and a graphite monochromator. Registration has been made stepwise in steps of 0.05 ° and counting time of 5 seconds in the angle from 20° to 100° 2θ. The research was carried on solid samples. Identification of crystalline phases present in the material were made using a database International Centre of Diffraction Data (PD4 + and COD Database).

At the scanning electron microscope metallographic research was made on metallographic specimen deeply etched in the light of the secondary electrons. Point EDX analysis was performed with a digital recording on the computer.

2.2. Microstructure of bronze in the cast state and after heat treatment

Figure 5 shows electron microscope images of the microstructure CuAl7Fe5Ni5W2Si2 bronze in the cast state, and the results point analysis of chemical composition in Table 2.

Added to aluminum bronze tungsten has the highest crystallization temperature (3422°C) of all elements contained in the chemical composition of the test bronze. Hence, it must be assumed that the phase containing a high concentration of tungsten will crystallize at high temperature mainly as a primary phase. From the presented analysis (Table 2, Figure 5a, points 2 and 3) shows that the microstructure of bronze are considered faceted intermetallic phases with a high content of tungsten (IM_W) 77.18 ÷ 82.65% .

At the phase boundary of these precipitates nucleate and grow the primary intermetallic phase κ_I of dendritic structure (Table 2, Figure 5a, point 1). Analysing the contribution of individual atomic elements in this phase can be stated that it has a composition similar to the type of iron silicide Fe_3Si and probably formed silicide M_3Si complex, where M=(Fe, Ni, Cu, Al).

The microstructure tested bronze also identified κ_{II} phase, which includes the following elements in an amount of about: 71.04% Fe, 16.09% Si, 6.23% Ni, 5.07% Cu, 1.57% Al. The nuclear share of individual elements that also this phase is share of elements close to the complex-type iron silicide M_3Si (Table 2, Figure 5b, point 1).

Bronze matrix is a α solution containing Cu within the 83.01÷ 83.62%, 7.61÷7.70% Al, 3.76÷4.31% Ni, 2.77÷3.11% W, 0.84÷ 1.77% Fe, 0.66÷0.85% Si (Table 2, Figure 5a and 5b, point 4). In the windows of analysis of chemical composition on the background of α phase can be seen a small spherical light phase precipitation probably κ_{IV}.

A significant part in the phase system α+ κ_{III} and eutectoid α+γ_2 is also α phase. In a mixture of phases α+κ_{III} concentration of the analyzed elements is approximately: 73.46% Cu, 9.80% Al, 9.34% Ni, 4.71% W, 1.85% Fe, 0.83, Si (Table 2, Figure 5a, point5).

In eutectoid α+γ_2, crystallizing in the last stage of the phase transitions tested bronze, and hence at relatively low temperatures were identified element concentration at the level: 80.95% Cu, 10.22% Al, 6.85% Ni, 1.11% Si and 0.86% W (Table 2, Figure 5b, point 3).

The results of X-ray phase analysis tested CuAl7Ni5Fe5W2Si2 bronze are shown in Figure 6 and Table 3. Unambiguously identified α-Cu phase, γ_2 (Cu_9Al_4) and α-Fe phase characteristic κ phase rich in iron.

The X-ray phase analysis also shows that the γ_2 phase diffraction lines coincide with the phases of the diffraction lines Cu_4Al_7Ni, Ni_5Al_3, α-Fe phase overlap with the reflections of Fe_3Al, FeAl, NiAl, and cannot be ruled Cu_3Al, CuAl, $Cu_{0.43}Fe_{0.57}$. However, due to the chemical composition tested characteristic bronze and aluminum bronze construction phase the presence of these phases is less likely. X-ray phase analysis has not identified all phases located in microstructure of the alloy. This is due to the construction of the first fine-grained microstructure, and second in receiving the new has not yet identified in current practice phase aluminum bronzes, for which no X-ray pattern yet been developed.

In Figure 7 (a÷d) shows the microstructure of CuAl7Fe5Ni5W2Si2 bronze observed on metallographic optical microscope, respectively:

- in the cast state (Fig. 7a),
- after quenching in 10% NaCl solution in water from a temperature of 1000°C, isothermally heated by the time:
  - 30 minutes (Fig. 7b),
  - 60 minutes (Fig. 7c),
  - 120 minutes (Fig. 7d).

As a result of observation of metallographic specimen of the bronze microstructure identified the following phases or their systems: IM_W\$\kappa_I$, κ_{II}, α, α+κ_{III}, α+κ_{IV}, α+γ_2 (Fig. 7a). At the metallographic specimen observed on metallographic microscope revealed no phase boundary between the primary intermetallic phase precipitates rich in tungsten, and the primary phase of κ_I growing on its borders. Hence the accepted for these phases a single indication in the form IM_W\$\kappa_I$.

The main task of the process of heating and annealing at 1000°C a tested bronze was to obtain in the microstructure of the secondary phase, β-saturated alloy additions. Regardless of time of isothermal annealing for hyperquenching bronze and then quenching in 10% NaCl solution in water, for all the analyzed annealing times: 30, 60 and 120 minutes, in the microstructure after the borders of the secondary β phase precipitation was achieved α phase. Regardless of time of isothermal annealing for hyperquenching bronze and then quenching in 10% NaCl solution in water, for all the analyzed annealing times: 30, 60 and 120 minutes, in the microstructure on the borders of the secondary β phase was achieved precipitation of α phase. With increasing annealing process, the primary precipitation of the phases IM_W\$\kappa_I$ undergo coagulation and coalescence (Fig. 7 b÷d). After 30 min annealing revealed the heterogeneity of the initial construction phase precipitates IM_W\$\kappa_I$ (Fig. 7 b). In the process of etching revealed the internal boundaries separating regions with very different chemical composition. Extending the isothermal annealing time to 60 minutes resulted in a significant homogenization of chemical composition of the phases (Fig. 7 c, d). Decreased number and length of internal borders in these phases, as disclosed in the process of etching.

Extending the isothermal annealing tested increases the number of secondary bronze disordered β phase, which is converted into an order-disorder transformation. Therefore, before quenching bronze, increases in the amount of the ordered β_1 phase in microstructure.

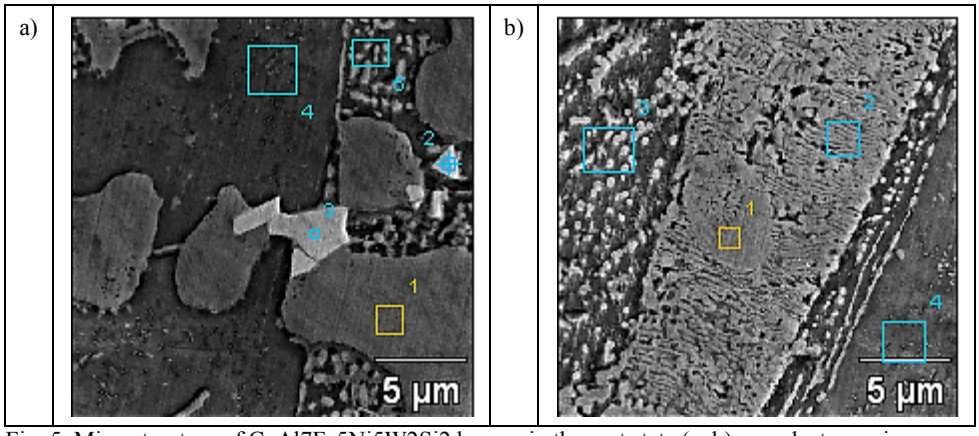

Fig. 5. Microstructure of CuAl7Fe5Ni5W2Si2 bronze in the cast state (a, b) - an electron microscope

Table 2.
The results of X-ray point analysis of chemical composition of phases in CuAl7Fe5Ni5W2Si2 bronze (cast state)

Fig. 5	Point	% Weight						Phase	Type of phase
		Al-K	*Si-K*	*Fe-K*	*Ni-K*	*Cu-K*	*W-M*		
a	*1*	1.38	14.24	74.13	7.20	3.04		*FeSiNiCuAl*	κ_I *Fe_3Si*
	2			14.30	1.58	6.94	77.18	*WFeCuNi*	*IM*
	3			14.52	2.83		82.65	*WFeNi*	*IM*
	4	7.70	0.66	1.77	3.76	83.01	3.11	α	*Solution*
	5	9.80	0.83	1.85	9.34	73.46	4.71	$\alpha+\kappa_{III}$	*Phase system*
		% Atom.							
		Al-K	*Si-K*	*Fe-K*	*Ni-K*	*Cu-K*	*W-M*		
	1	2.49	24.66	64.55	5.97	2.33		*$Fe_{2.62}Si_{1.00}Ni_{0.24}$ $Al_{0.10}Cu_{0.09}$*	κ_I *Fe_3Si*
	2			31.53	3.32	13.44	51.71		*IM*
	3			34.31	6.37		59.32		*IM*
	4	16.51	1.35	1.83	3.71	75.61	0.98	α	*Solution*
	5	20.56	1.67	1.88	9.01	65.43	1.45	$\alpha+\kappa_{III}$	*Phase system*
b		% Weight							
		Al-K	*Si-K*	*Fe-K*	*Ni-K*	*Cu-K*	*W-M*		
	1	1.57	16.09	71.04	6.23	5.07		*FeSiNiCuAl*	κ_{II} *Fe_3Si*
	3	10.22	1.11		6.85	80.95	0.86	$\alpha+\gamma_2$	*Phase system*
	4	7.61	0.85	0.84	4.31	83.62	2.77	α	*Solution*
		% Atom.							
		Al-K	*Si-K*	*Fe-K*	*Ni-K*	*Cu-K*	*W-M*		
	1	2.79	27.42	60.89	5.08	3.82		*$Fe_{2.22}Si_{1.00}Ni_{0.19}$ $Cu_{0.14}Al_{0.10}$*	κ_{II} *Fe_3Si*
	3	20.89	2.19		6.44	70.24	0.26	$\alpha+\gamma_2$	*Phase system*
	4	16.29	1.75	0.87	4.24	75.98	0.87	α	*Solution*

IM – intermetallic phases
Fig.5 b – lack of analysis for point 2

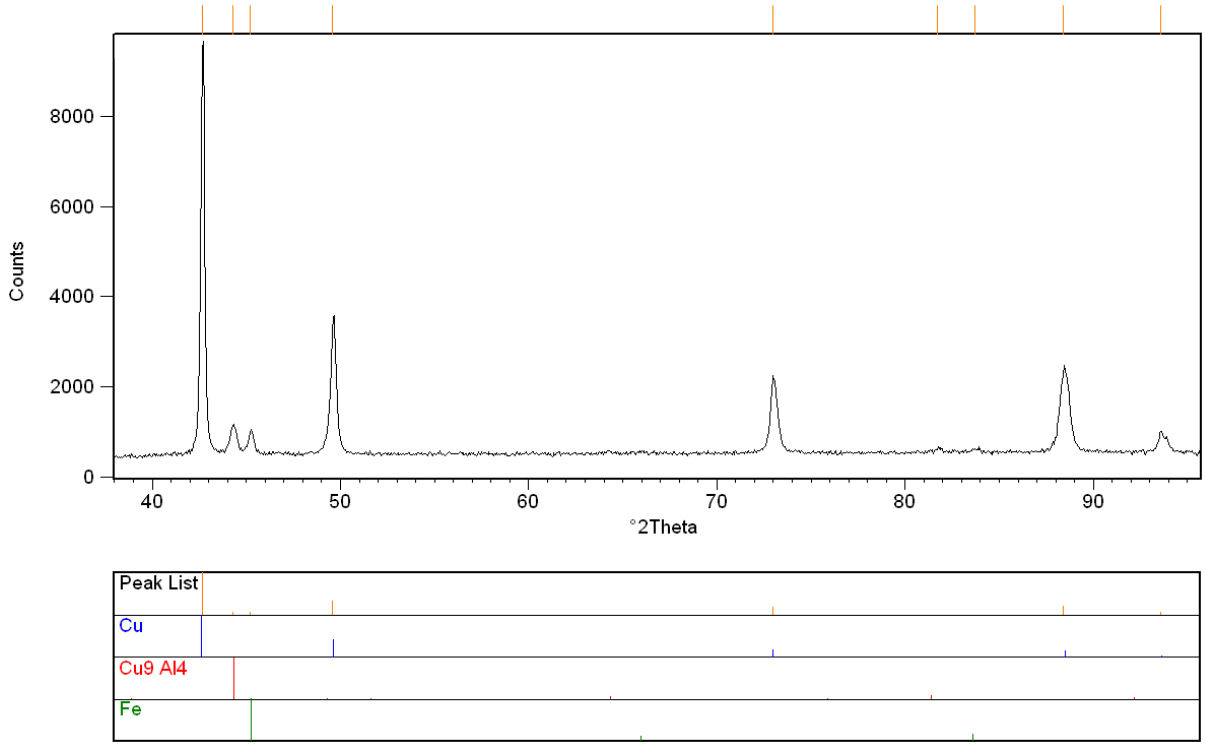

Fig. 6. X-ray diffraction CuAl7Ni5Fe5W2Si2 samples in the cast state

Table 3.
The results of X-ray phase analysis of CuAl7Ni5Fe5W2Si2 samples in the cast state

d_{hkl} [Å]	Int.	α-Cu (04-004-2760) Cubic, *Fm-3m* (225) a_0 = 3.6528 Å			Cu_9Al_4 (04-003-1893) Cubic, *P-43m* (215) a_0 = 8.7023 Å			α-Fe (04-013-9776) Cubic, *Im-3m (229)* a_0 = 2.83 Å		
		d_{hkl} [Å]	Int.	*h k l*	d_{hkl} [Å]	Int.	*h k l*	d_{hkl} [Å]	Int.	*h k l*
2.12	100	2.11	100	1 1 1						
2.04	6				2.051	100	3 3 0			
2.00	6							2.00	100	1 0 0
1.84	32	1.82	43	2 0 0	1.855	4	3 3 2			
1.30	20	1.29	17	2 2 0						
1.18	1				1.184	8	7 2 1			
1.15	1							1.16	17	2 1 1
1.10	20	1.10	16	3 1 1						
1.06	6	1.05	4	2 2 2	1.071	5	7 4 1			

In the study of the chemical composition of bronze in the microstructure after quenching, martensite is formed both β'and β_1'. The share of martensite - type β_1' in the microstructure increases with increasing bronze isothermal annealing time. Due to the difficulty of distinguishing between areas metallographic specimen martensite β'and β_1' in Figure 7 (b÷d) are designated areas and the symbol "m" - martensite.

In addition to martensite in the microstructure revealed areas of bainite precipitates, consisting of phases: α' (saturated α phase) + nontransform β phase (β/β_1) + and martensite β'/β_1', labeled in Figure 7 (b÷d) the letter "b".

Characteristic of heat treatment CuAl7Ni5Fe5W2Si2 bronze to create a large quantity of very fine precipitates, most likely type of intermetallic phases κ_V. Precipitations of these have been identified mainly on the background of martensitic and bainitic matrix. This probably indicates that it builds in the process of cooling at the lowest temperature range close to ambient temperature. Intermetallic κ_V phases were not identified on the background α phase.

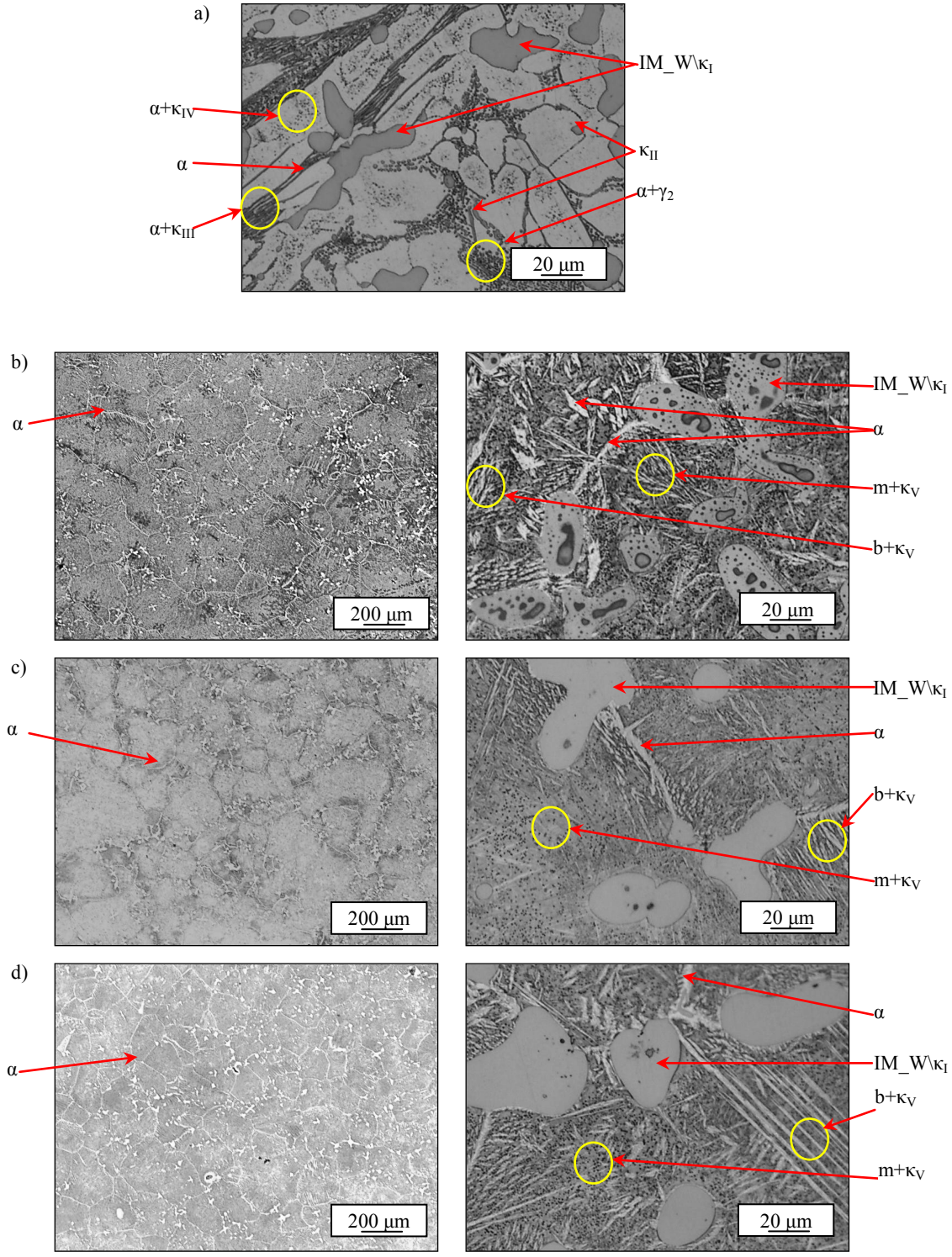

Fig. 7. Microstructure of CuAl7Fe5Ni5W2Si2 bronze: a) the cast state, b) after annealing at 1000 ˚C for 30 min and quenching in 10% NaCl solution in water, c) after annealing at 1000˚C for 60 min and quenching in 10% NaCl solution in water, d) after annealing at 1000 ˚C in 120 minutes and quenching in 10% NaCl solution in water m - martensite ($\beta'\backslash\beta_1'$), b - bainite ($\alpha'+\beta/\beta_1+\beta'\backslash\beta_1'$)

The results of X-ray phase analysis tested bronze after quenching from 1000°C, annealing for 30 minutes are shown in Figure 8 and Table 4.

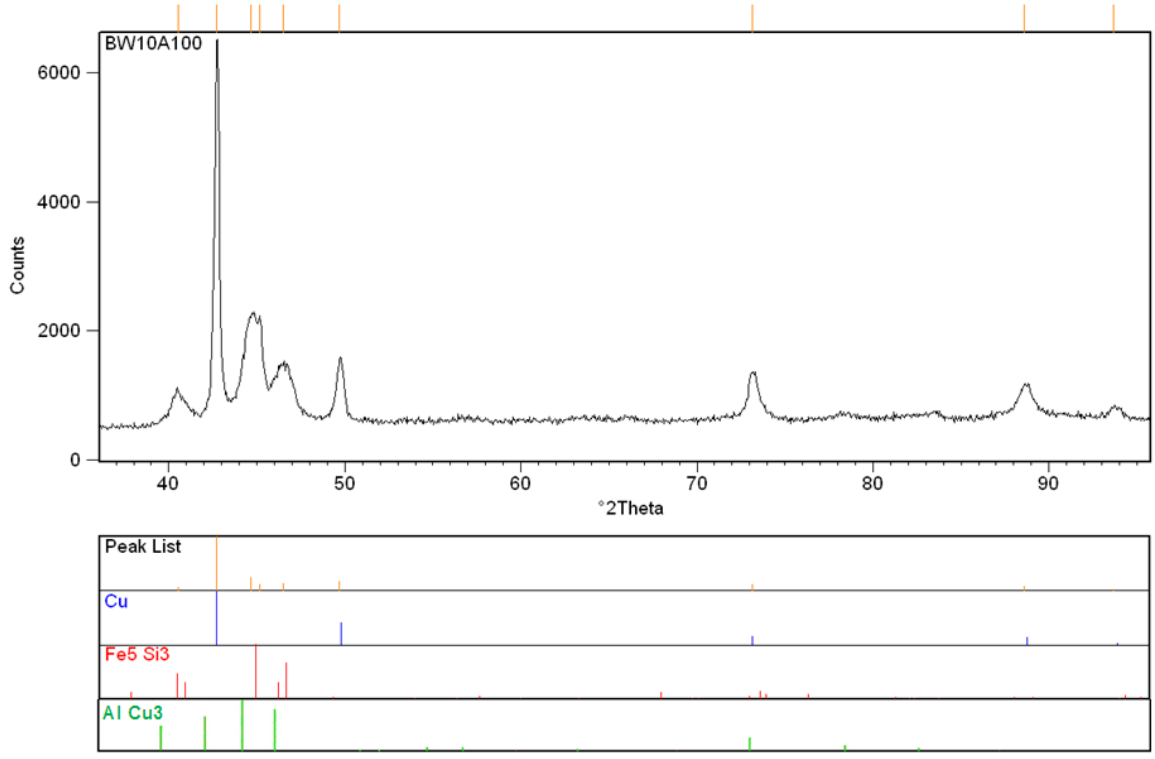

Fig. 8. X-ray diffraction CuAl7Fe5Ni5W2Si2 sample after annealing at 1000°C for 30 min and cooling in 10% NaCl solution in water

Table 4.
The results of X-ray phase analysis CuAl7Fe5Ni5W2Si2 sample after annealing at 1000°C for 30 min and cooling in 10% NaCl solution in water

d_{hkl} [Å]	Int.	Fe_5Si_3 (04-07-8007) Heksagonal, *P63/mcm* (193) a_0 = 6.755 Å, c_0 = 4.717 Å			α-Cu (04-003-2430) Cubic, *Fm-3m* (225) a_0 = 3.645 Å			Cu_3Al (00-028-0005) Orthorhombic, P a_0 = 4.494 Å, b_0 = 5.189 Å, c_0 = 46.61 Å		
		d_{hkl} [Å]	Int.	*h k l*	d_{hkl} [Å]	Int.	*h k l*	d_{hkl} [Å]	Int.	*h k l*
2.22	7	2.21	47	2 1 0				2.237	50	2 0 2
		2.19	31	1 0 2						
2.12	100				2.10	100	1 1 1	2.114	65	0 0 22
2.03	26							2.021	100	1 2 10
2.01	12	2.00	100	2 1 1						
1.95	14	1.95	31	3 0 0				1.947	80	2 0 12
		1.93	67	1 1 2						
1.83	17	1.84	4	2 0 2	1.82	43	2 0 0			
1.29	11	1.29	5	3 2 1	1.29	17	2 2 0	1.295	25	0 4 2
		1.28	15	2 1 3						
1.10	8	1.11	3	4 2 0	1.10	16	3 1 1	1.120	2	3 2 21
1.06	3	1.05	8	5 0 2	1.05	4	2 2 2			

Unambiguously identified α-Cu phase and Fe5Si3. Probably in the process of isothermal annealing bronze by diffusion, comes to the enrichment of the Si phase system IM_W\κ_I. Thus, primary created κ_I phase having the chemical composition similar to the complex-type iron silicide M_3Si rebuilds its lattice to a lattice similar to a complex type M_5Si_3 silicide. The X-ray phase analysis shows the relatively weak diffraction lines characteristic matching for phase β. This is due primarily fine-grained metal matrix structure. Get a new, not yet identified in current practice phase aluminum bronzes are not identified because of the non-existence of X-ray patterns yet.

2.3. Sample temperature during heat treatment

Figure 9 shows the temperature characteristics of a representative sample of CuAl7Fe5Ni5W2Si2 bronze a function of time, for different stages of heat treatment and the time of isothermal annealing sample τ = 60 min (3600 s).

In the first stage of heat treatment - heating of the sample together with the furnace to a temperature T = 1000°C (stage T1) followed by dissolution of phase or phase systems according to their phase transition temperature. With the increasing temperature of the bronze sample is first dissolved eutectoid $\alpha+\gamma_2$, creating a highly saturated β phase Al - according to the phase equilibrium diagram (Fig. 1) about 13.8% Al. Next, the soluble phase system, respectively $\alpha+\kappa_{IV}$, α+κIII first creating a saturated admixtures (Fe, Ni, Si, W) α phase. Saturated α phase additions and α phase was formed without the participation of intermetallic phases and κ_{IV} and κ_{III} transformed into β phase has a lower concentration of Al than the β phase formed from the dissolution of eutectoid, but with a higher concentration of additions alloyed bronze. In the final stage of heating at temperatures above 950°C, begins dissolving in the β phase intermetallic phases κ_{II}. Probably at the stage of heating, the process of their total dissolution in the β phase does not occur until the end, because of the high temperature of dissolution and a relatively high rate of heating the sample.

At this scale of temperature and time (Fig. 9) it is difficult to identify the characteristic changes of the sample temperature, respectively, during the annealing (stage T2 - isothermal annealing), hyperquenching and quenching bronze (stage T3 - cooling in ambient air and T4 stage - cooling in 10% NaCl solution in water). Figure 10 shows representative characteristics of temperature changes during the isothermal annealing bronze sample at a constant temperature of t=1000°C for 3600 s. There was a decrease of the temperature characteristic bronze samples during the annealing process in the studied range of isothermal annealing time (30, 60 and 120 min.). The presented characteristics t=f(τ) for a sample of bronze in the furnace that, after heating the furnace and the sample to a temperature of 1000°C, there was a gradual decrease in temperature of the sample to about 996°C. Decrease of the temperature of the sample is associated with absorption of heat by the phase existing in bronze at 1000°C, necessary for the occurrence of the following diffusion processes:

- completion of phases dissolution κ_{II} in β phase,
- homogenization of additions in β phase,
- a partial transformation of disordered β phase in the ordered β_1 phase,
- homogenization of additions in intermetallic phases of the primary IM_W\κ_I,
- the primary IM_W\κ_I phases coagulation,
- coalescence of primary phases IM_W\κ_I.

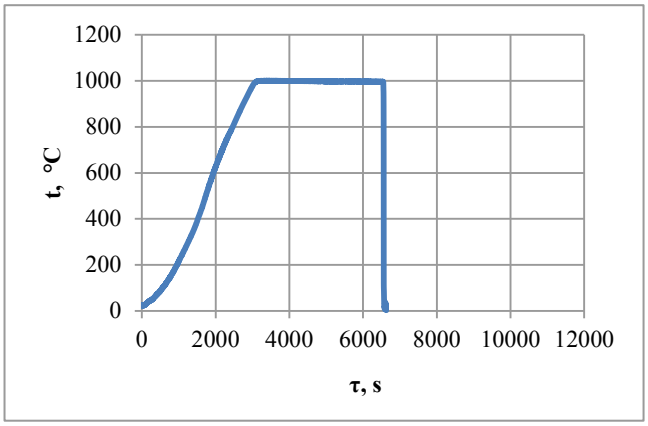

Fig. 9. The temperature of the CuAl7Fe5Ni5W2Si2 bronze samples during heat treatment - quenching from 1000°C after annealing at 3600 s
(annealing time of sample 3000 s)

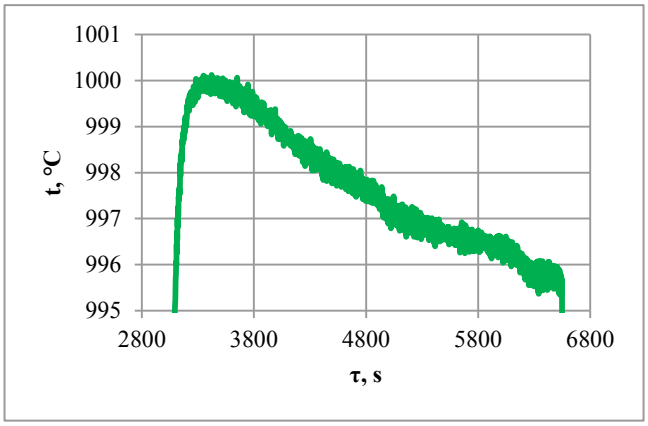

Fig. 10. Bronze sample temperature during the annealing at 1000°C for 3600 s

In Figure 11 presents a summary of characteristics t=f(τ) (after taking into account the time shift - to align the start of the cooling operation) of the bronze samples tested on the cooling (T3 and T4). At constant coolant properties (chemical composition, thermophysical properties) were obtained with very different characteristics located t=f(τ) of the samples.

For the curves t=f(τ) changes in sample temperature during heat treatment was determined dt/dτ=f '(τ) - the first derivative of temperature T after time τ. The designated derivative is characterized by of sample cooling rate during its intensive cooling.

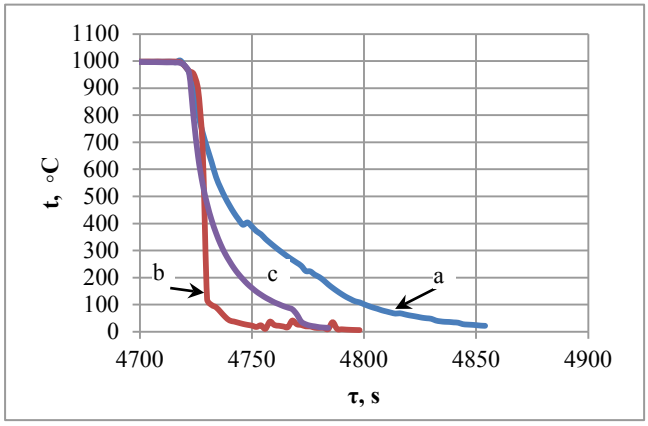

Fig. 11. Characteristics of t=f(τ) samples CuAl7Fe5Ni5W2Si2 bronze during heat treatment
- quenching from a temperature of 1000°C
after annealing at:
a) 1800 s, b) 3600 s, c) 7200 s

The highest cooling rate tested of bronze sample was obtained after annealing it in 60 minutes and it amounted to -135.6°C/s. Then, after 120 min annealing, and it amounted to -46.3°C/s, cooling rate and the lowest -36.8°C/s of sample was obtained after 30 min annealing.

It was determined, in the temperature range from 1000°C to 100°C an average cooling rate of tested bronze samples, for samples annealing at:

- 1800 s - 4.5°C/s,
- 3600 s - 26.7°C/s,
- 7200 s - 6.7°C/s.

a)

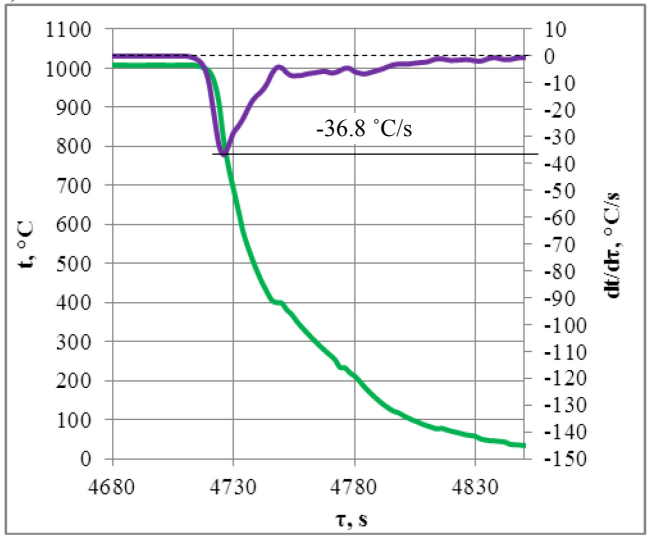

b)

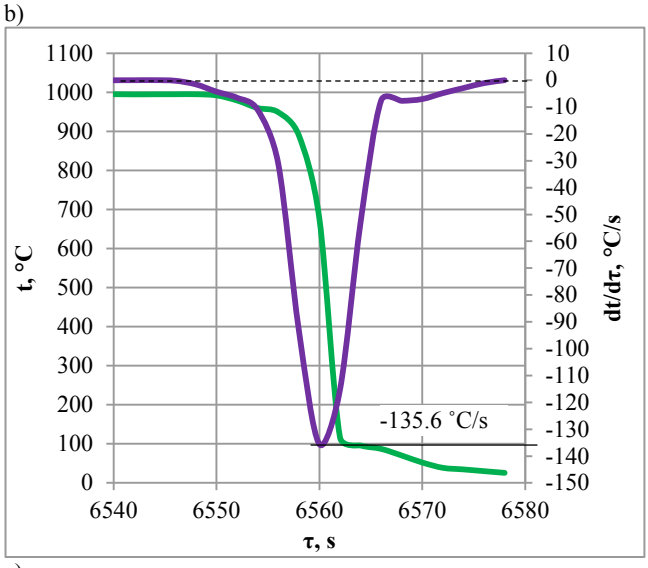

c)

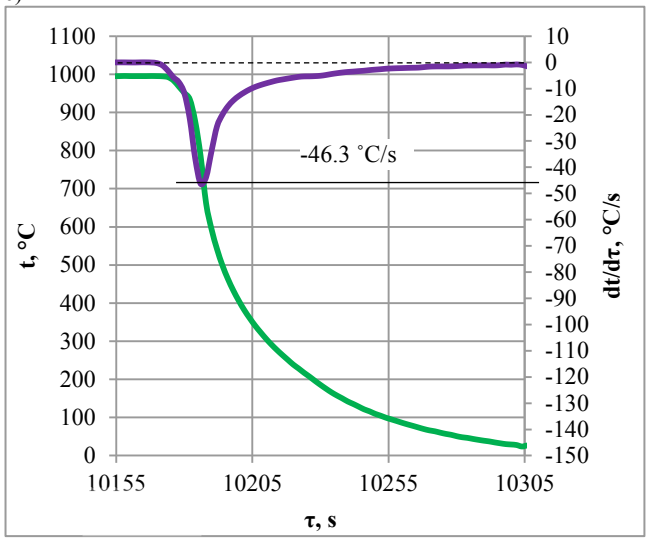

Fig. 12. Characteristics of t=f(τ) and dt/dτ=f '(τ) samples CuAl7Fe5Ni5W2Si2 bronze during heat treatment - quenching from a temperature of 1000 ° C after annealing at:
a) 1800 s, b) 3600 s, c) 7200 s

Characteristic changes in the course tested bronze sample temperature during cooling (stage T3 and T4 heat treatment process), and consequently the rate of cooling is primarily due to:

- change of thermal conductivity λ and specific heat Cp bronze matrix, ie phases: α, α', β, β_1, β', β_1'caused varying degrees of supersaturation elements (Figure 1 and Figure 2) significantly changing the thermal conductivity and specific heat of copper and, consequently, in her rich phases,
- percentage change in the microstructure of the individual components of the matrix,
- generation of crystallization heat phases formed in the processes of diffusion (α, α').

2.4. Quantitative analysis of the microstructure and mechanical properties of bronze

Statistically developed the results of digital image analysis of the microstructure CuAl7Fe5Ni5W2Si2 bronze, for the average values of the percentage of the individual components of the microstructure and microhardness $HV_{0.1}$, respectively is shown in Figure 13 (a,b). Table 5 shows, respectively, average values of these quantities and their standard deviation.

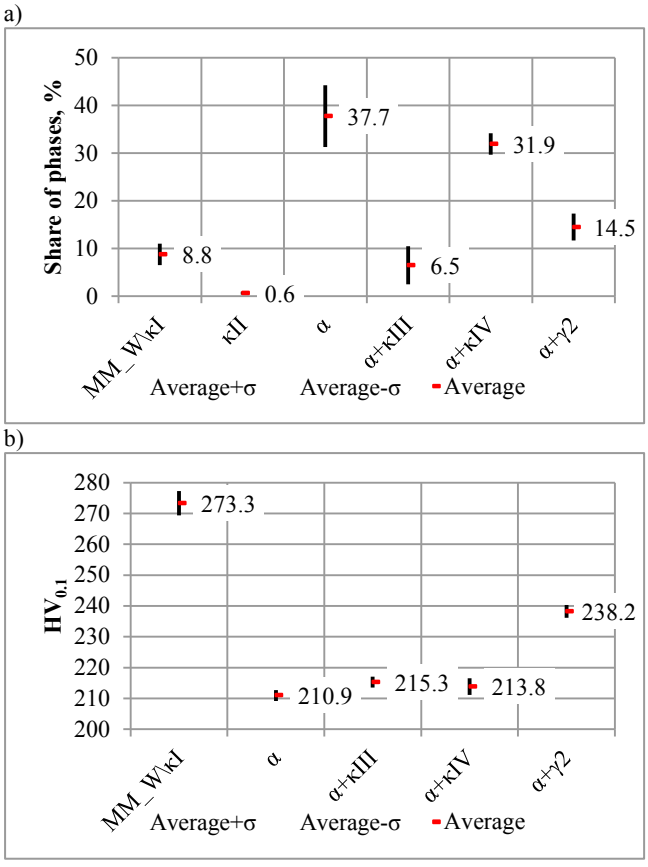

Fig. 13. Share (a) and microhardness $HV_{0.1}$ (b) of the various phases and their systems in the microstructure CuAl7Fe5Ni5W2Si2 bronze in the cast state

The largest share in the microstructure tested bronze has obviously α phase and α phase with intermetallic phases κ_{III} and κ_{IV} type. Together they have 76.1% share of the order, α phase and α phase with κ-type phases have similar hardness in the range 211 to 215 $HV_{0.1}$. Harder phase system, with an average of 238.5 $HV_{0.1}$ microhardness, is a mixture of eutectoid $\alpha+\gamma_2$ occupying with about 14.5% of the area.

In the bronze CuAl7Fe5Ni5W2Si2 microstructure (Fig. 7a) identified a relatively small precipitations of intermetallic phase κ_{II}, which falls to the lowest share in the microstructure of the order of 0.6%, with an area average of 10.3 ± 7.8 μm^2, which is equivalent to the circle diameter of 3.39±1.25 μm, it was impossible to measure the microhardness $HV_{0.1}$. Therefore, the combination of microhardness phases (Fig. 13b) omitted microhardness of intermetallic κ_{II} phases.

Hardest components of the microstructure of bronze are tested the primary precipitation of phases, intermetallic phases rich in tungsten and surrounding dendritic κ_I phases precipitates, similar in its chemical composition to the type of iron silicide Fe_3Si. They participated in microstructure of bronze of the order of 8.8% and the average microhardness of the order of 273.3 $HV_{0.1}$.

Table 5.
The average values and standard deviation σ of measurements, share percentage of phases in microstructure, and their microhardness $HV_{0.1}$ in CuAl7Fe5Ni5W2Si2 bronze in the cast state

	IM_W\κ_I	κ_{II}	α	$\alpha+\kappa_{III}$	$\alpha+\kappa_{IV}$	$\alpha+\gamma_2$
	Share of phases, %					
Average	8.8	0.6	37.7	6.5	31.9	14.5
σ	2.22	0.32	6.50	4.00	2.23	2.82
	$HV_{0.1}$					
Average	273.3	-	210.9	215.3	213.8	238.2
σ	3.96	-	1.76	1.76	2.69	2.11

Due to the fact that during the heat treatment tested bronze on the borders of the secondary β phases formed during isothermal annealing, precipitated α phase (Fig. 7 b÷d), and after precipitation is not subject to further transformations, enables the identification of grain size β phase prior to its transformation into martensite (β'\β1') and bainite (α'+β\β1+β'\β_1'). The change of grain surface area β phase (Sap_β) and the length of the intergranular phase boundaries β (Lpb_β), depending on time of isothermal annealing (τ_ia) of bronze samples are shown in Figure 14 and 15, and descriptive statistics of the quantities in Table 6 and 7.

Extending time of isothermal annealing bronze in the range 30 to 120 min causes continuous decrease of the surface area formed β phases (Fig. 14, Tab. 6). There is a size reduction of the β phase grains, indicates the median value of which decreases with increasing time τ_ia.

After 60 min of isothermal annealing the β phase formed grains with boundaries which are the most developed. With the general trend of size reduction grain β phase, with increasing time τ_ia, increase the length of the grain boundaries indicates a greater heterogeneity in size grains in the in bronze microstructure, heat treated under these conditions (Fig. 7 c). For very small grains, grains also were identified about a larger surface area and greatly developed interphase boundary. Extending the annealing time of 120 min possible to obtain grains of β phase with the shortest grain boundaries (Fig. 15, Tab. 7).

Percentage change in the content of α phase and the width of the precipitates at grain boundaries are shown in Figure 16 (a, b) and 17. Descriptive statistics of these quantities are shown in Table 8 and 9.

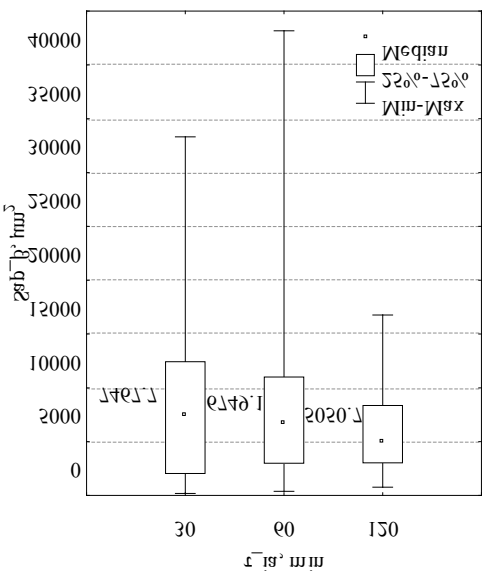

Fig. 14. The surface area of the phase β (Sap_β) depending on the annealing time (τ_ia) samples of CuAl7Fe5Ni5W2Si2 bronze

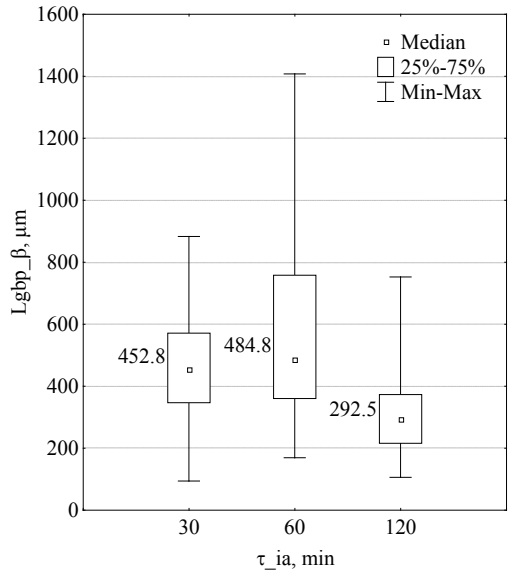

Fig. 15. The length of the interphase grains boundary of β phase (Lgbp_β) depending on the annealing time (τ_ia) samples of CuAl7Fe5Ni5W2Si2 bronze

Table 6.
Descriptive statistics for the measurement grains surface area of the β phase (Sap_β, μm^2) in microstructure of the CuAl7Fe5Ni5W2Si2 bronze, after isothermal annealing time (τ_ia, min)

τ_ia, min	Average	N significant	Median	Minimum	Maximum	25 Percentile	75 Percentile	Standard dev. σ	Spread	Quartile spread	Σ
30	8410.9	198	7467.7	179.1	33317.1	2028.6	12421.8	6587.0	33138.0	10393.2	1665365.6
60	8642.7	189	6749.1	372.8	43160.8	2983.6	10995.0	8718.1	42788.0	8011.4	1633461.0
120	6006.1	258	5050.7	758.4	16760.8	3021.3	8357.0	3870.7	16002.4	5335.6	1549568.0

Table 7.
Descriptive statistics for measuring the length of the interphase grain boundary β phase (Lgbp_β, μm) in microstructure of the CuAl7Fe5Ni5W2Si2 bronze, after isothermal annealing time (τ_ia, min)

τ_ia, min	Average	N significant	Median	Minimum	Maximum	25 Percentile	75 Percentile	Standard dev. σ	Spread	Quartile spread	Σ
30	458.7	198	452.8	94.6	883.6	347.2	571.7	161.2	789.0	224.5	90829.0
60	542.1	189	484.8	169.8	1408.0	360.7	758.6	242.0	1238.2	397.9	102460.7
120	303.1	258	292.5	106.5	753.0	216.4	373.5	115.7	646.5	157.1	79109.4

In the bronze microstructure formed after quenching, the relatively small amount of α phase precipitates on the borders of the secondary β phase (α_b), and inside it (α_ig). In the microstructure of the tested bronze after heat treatment, the average percentage of α phase at grain boundaries separate secondary β phase change within the α_b=1.6÷2.1%, and within it α_ig=0.2÷4.9%.
Summarily (α_b+α_ig) the least amount of α phase is obtained after the isothermal annealing time τ_ia=60 min 1.8% α and the highest after 120 minutes of annealing 7.0% α (Fig. 16 (a, b), tab. 8). A similar character of changes was also observed when measuring the width of α phase precipitates at grain boundaries Swf_α β phase (Fig. 17, Tab. 9). Because of the relatively small average width of the α phase precipitates at the grain boundaries β phase, the order of 0.51÷0.65 μm (Table 9), was not measured, $HV_{0.1}$ microhardness of this phase.

The area of primary precipitates of intermetallic phases IM_W\κ$_I$ and the length of their boundaries, respectively, are shown in Figure 18 and 19, and descriptive statistics measurement of the quantities in table 10 and 11.
In the microstructure of the tested bronze in the cast state there were conglomerates of primary intermetallic phases and IM_W\κ$_I$, with varying concentrations of elements contained in their chemical composition and in different proportions relative to each other. During annealing bronze, followed by the mutual diffusion gradually dissolving, and with increasing annealing time within

the homogenized composition of primary phases (Fig. 7b÷d). Prolongation of the isothermal annealing of samples tested bronze increases the surface area of primary precipitates of intermetallic phases IM_W\κ$_I$, creating a common area, close to its lattice structure of iron silicide Fe_5Si_3 (Fig. 8, Tab. 4).

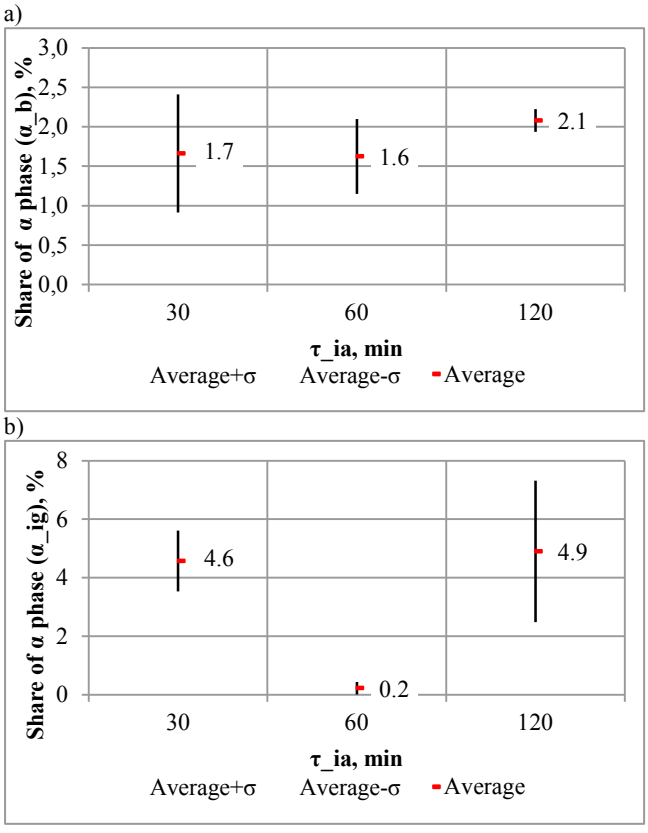

Fig. 16. The share of α phase, depending on the annealing time (τ_ia) in the microstructure of samples CuAl7Fe5Ni5W2Si2 bronze:
a) α_b - on the intergranular border of secondary β phase,
b) α_ig - inside the grains of secondary β phases

Table 8.
The average values and standard deviation σ of measurements of the percentage of α phase (α_b, α_ig) in the microstructure CuAl7Fe5Ni5W2Si2 bronze after isothermal annealing time τ_ia

α_b	τ_ia, min		
	30	60	120
	Share of α phase, %		
Average	1.7	1.6	2.1
σ	0.75	0.47	0.14
α_ig	τ_ia, min		
	30	60	120
	Share of α phase, %		
Average	4.6	0.2	4.9
σ	1.04	0.20	2.42

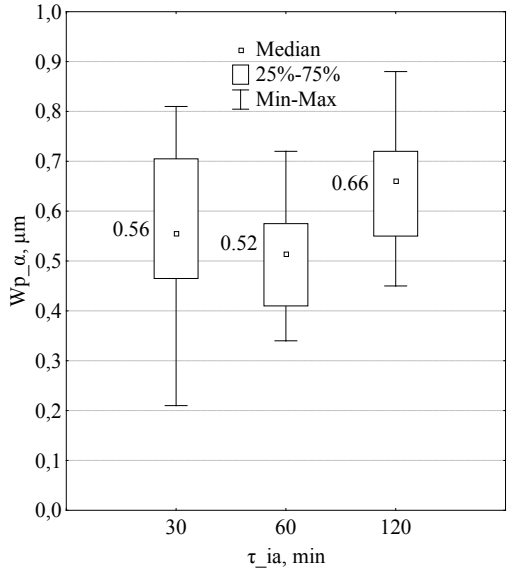

Fig. 17. Width of the precipitates α phase (Wp_α) depending on the annealing time (τ_ia) in the microstructure of samples CuAl7Fe5Ni5W2Si2 bronze

Table 9.
Descriptive statistics for measuring the width of the precipitates α phase (Wp_α, um) at the grain boundaries of secondary β phase in the microstructure CuAl7Fe5Ni5W2Si2 bronze after annealing (τ_ia, min)

τ_ia, min	Average	N significant	Median	Minimum	Maximum	25 Percentile	75 Percentile	Standard dev. σ	Spread	Quartile spread	Σ
30	0.57	36	0.56	0.21	0.81	0.47	0.71	0.17	0.60	0.24	30
60	0.51	36	0.52	0.34	0.72	0.41	0.58	0.12	0.38	0.17	60
120	0.65	24	0.66	0.45	0.88	0.55	0.72	0.13	0.43	0.17	120

Admixtures saturate the metallic bronze matrix (β, β_1), such as Al, Fe, Ni, W, and especially Si, diffuse for the primary phases and expand them at the expense of the size of the phases β and β_1. The average value of the surface area varies in the range 13.6÷15.9 μm_2 (Fig. 20a, Tab. 12).

After annealing bronze by the time 120 min, the microstructure of bronze are present a single, very large the primary phase precipitates, which had absorbed as a result of coalescence of the adjacent lower primary phase precipitates. While a small value of the median 2.5 μm^2, a collection of measurements of the surface area of the primary phase, is associated with a growing number of primary phase precipitates κ_I, probably without the nucleating high tungsten intermetallic IM_W phases, dissolve in the matrix β and β_1, like intermetallic phases κ_{II}, but much from them slowly. Evidence of this is also moving percentiles, respectively, percentile 25 in the direction of lower values of the surface area of intermetallic phases, and the percentile 75 in the direction of higher values of measurements of the field.

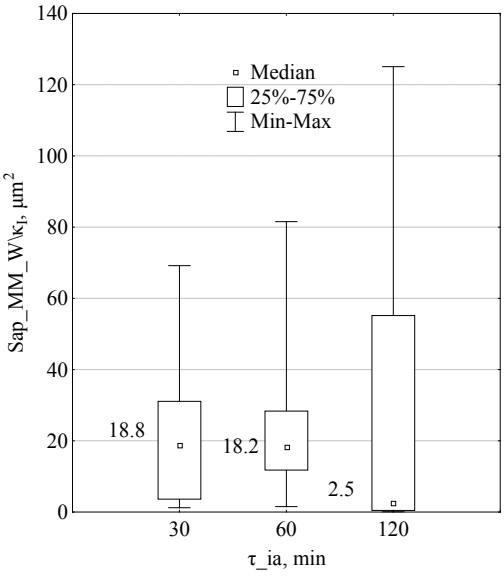

Fig. 18. The area of the precipitates of primary intermetallic IM_W\$\kappa_I$ phases (Sap_IM_W\$\kappa_I$) depending on the annealing time (τ_ia) in the microstructure of samples CuAl7Fe5Ni5W2Si2 bronze

Coagulation of primary intermetallic phases is also confirmed by measurements of the length of the interface of primary IM_W\κ_I phases. With increasing annealing time τ_ia decreasing both the average length of the primary phase boundary, and their median (Fig. 19, Tab. 11).

The percentages of primary phases, bainite and martensite in the microstructure of the tested bronze and their microhardness $HV_{0.1}$ are shown in Figures 20 (a,b)÷22 (a,b). Average values measurements of the percentage of phases and their microhardness and corresponding to the measured standard deviation are shown in Tables 12÷14.

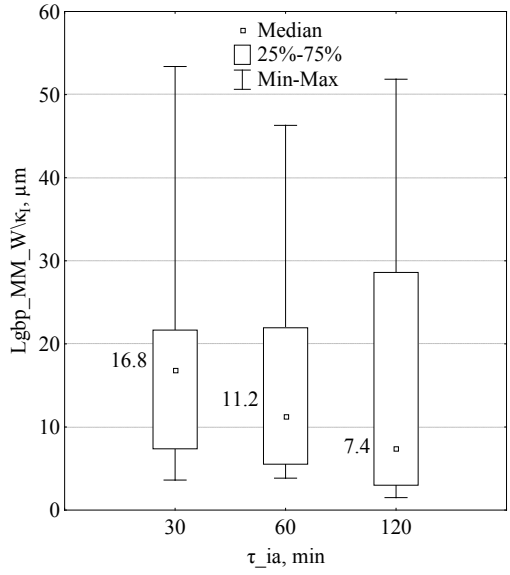

Fig. 19. The length of the grain boundaries of primary intermetallic phases IM_W\κ_I (Lgbp_ IM_W\κI) depending on the annealing time (τ_ia) in the microstructure of samples CuAl7Fe5Ni5W2Si2 bronze

The share of phases IM_W\κ_I in the microstructure tested bronze with increasing time of isothermal annealing changes in a relatively small range from 13.6% to 15.9% (Fig. 20a, Tab. 12). The smallest amount of the primary intermetallic phases were obtained after annealing tested bronze for 60 minutes, and the highest after 120 minutes.

Table 10.
Descriptive statistics for measuring the surface area the primary precipitates of intermetallic phases IM_W\$\kappa_I$ (Sap_IM_W\$\kappa_I$, μm^2) depending on the annealing time (τ_ia, min) in the microstructure of samples CuAl7Fe5Ni5W2Si2 bronze

τ_ia, min	Average	N significant	Mediana	Minimum	Maximum	25 Percentile	75 Percentile	Standard dev. σ	Spread	Quartile spread	Σ
30	20.8	56	18.8	1.2	69.2	3.6	31.1	17.9	68.0	27.5	581.1
60	22.9	48	18.2	1.5	81.5	11.8	28.3	18.9	80.0	16.6	549.8
120	27.7	30	2.5	0.1	125.1	0.5	55.2	43.1	125.0	54.7	414.8

Table 11.
Descriptive statistics for measuring the length of boundary of the intermetallic primary IM_W\κI phases precipitates (Lgbp_IM_W\κI, um), depending on the annealing time (τ_ia, min) in the microstructure of samples CuAl7Fe5Ni5W2Si2 bronze

τ_ia, min	Average	N significant	Mediana	Minimum	Maximum	25 Percentile	75 Percentile	Standard dev. σ	Spread	Quartile spread	Σ
30	16.3	28	16.8	3.6	53.4	7.4	21.7	10.8	49.8	14.3	455.7
60	15.5	24	11.2	3.8	46.3	5.5	21.9	11.4	42.5	16.4	372.1
120	15.3	15	7.4	1.5	51.8	3.0	28.6	16.6	50.4	25.6	229.9

With the extending of time τ_ia definitely increases the average microhardness of the primary phases precipitates of 592.7÷724.6 $HV_{0.1}$ (Fig. 20b, Table 13).

After isothermal annealing for 60 minutes samples CuAl7Fe5Ni5W2Si2 bronze were obtained in the least amount of bainite microstructure of about 11.9% (Fig. 21a, tab. 12). The greatest amount of bainite in tested bronze, for the analyzed annealing time 27.5% was obtained after lengthening τ_ia time to 120 minutes. Microhardness of bainite varied in the range of 316.7÷331.6 $HV_{0.1}$.

a)

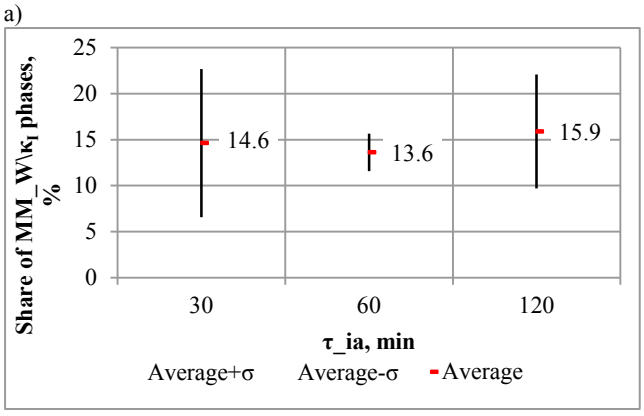

b)

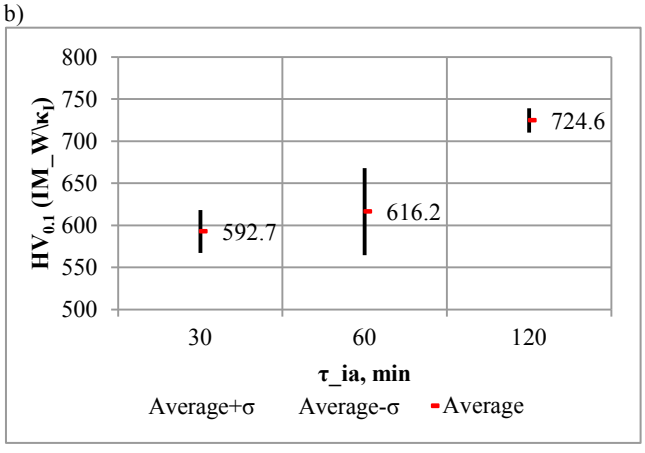

Fig. 20. The share the primary precipitates of intermetallic phases IM_W\κI (a) and microhardness $HV_{0.1}$ (b) depending on the annealing time (τ_ia) in the microstructure of samples CuAl7Fe5Ni5W2Si2 bronze

Table 12.
The average values and standard deviation σ measurement of the percentage share of phases IM_W\κI and microhardness $HV_{0.1}$ in the microstructure CuAl7Fe5Ni5W2Si2 bronze after annealing in τ_ia time

τ_ia, min	30	60	120
Share of IM_W\κI phases, %			
Average	14.6	13.6	15.9
σ	8.04	2.04	6.21
$HV_{0.1}$			
Average	592.7	616.2	724.6
σ	25.56	51.81	14.33

Microstructure of bronze after annealing at τ_ia=60 min was characterized by the highest microhardness of bainite. In the case of martensite obtained, both the largest share of 72.6%, how and the highest microhardness 401.3 $HV_{0.1}$ in the tested bronze, after isothermal annealing for 60 min (Fig. 22a, tab. 14). However, after annealing bronze for 120 minutes, the amount of martensite decreases to about 49.7% and is characterized by the lowest microhardness of the order of 366.5 $HV_{0.1}$.

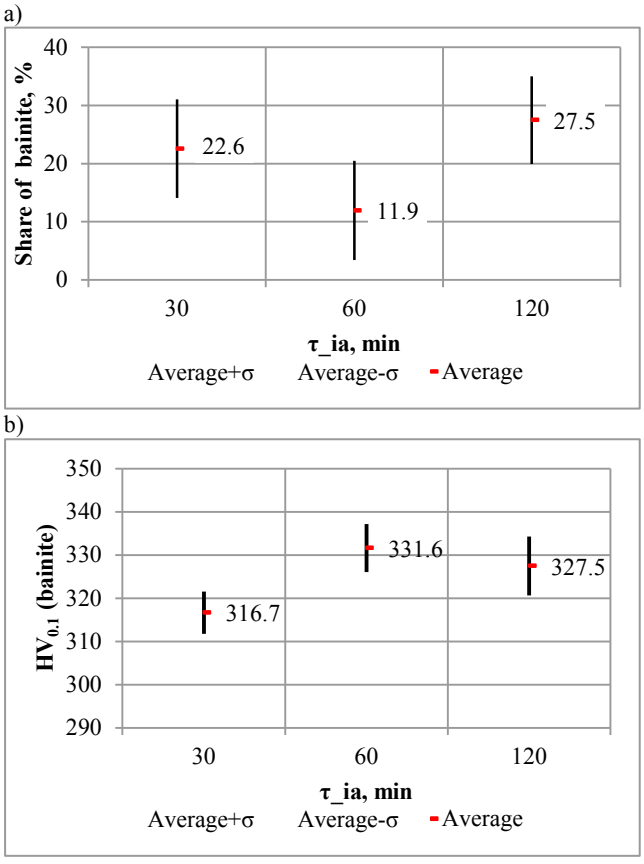

Fig. 21. The share of bainite α'+β\β$_1$+β'\β$_1$' (a) and the microhardness $HV_{0.1}$ (b) depending on the annealing time (τ_ia) in the microstructure of samples CuAl7Fe5Ni5W2Si2 bronze

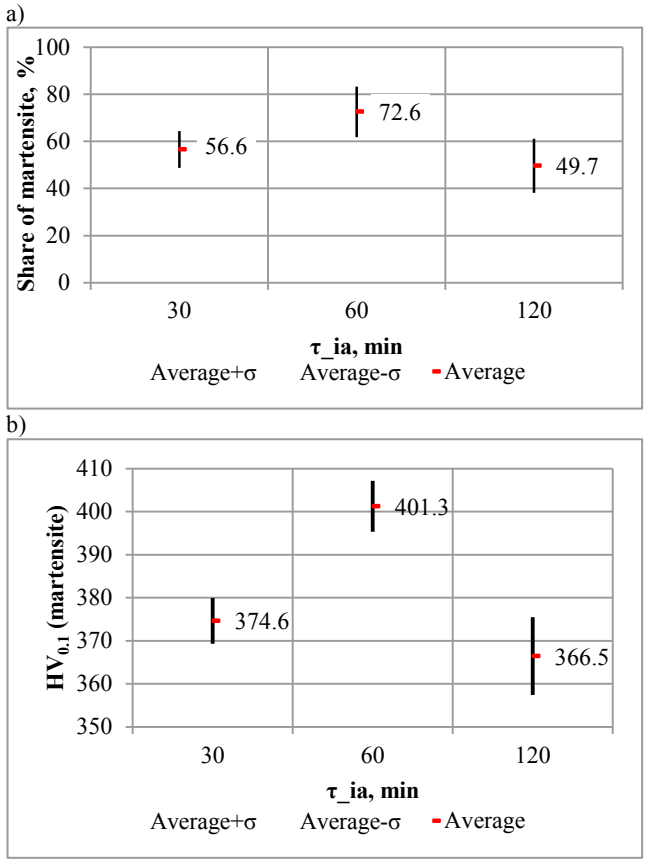

Fig. 22. The share of martensite β'\β$_1$' (a) and the microhardness $HV_{0.1}$ (b) depending on the annealing time (τ_ia) in the microstructure of samples CuAl7Fe5Ni5W2Si2 bronze

Table 13.
The average values and standard deviation σ, measuring the share of bainite α'+β\β$_1$+β'\β$_1$'and its microhardness $HV_{0.1}$ in the microstructure CuAl7Fe5Ni5W2Si2 bronze after annealing τ_ia time

τ_ia, min	30	60	120
Share of bainite, %			
Average	22.6	11.9	27.5
σ	8.48	8.52	7.54
$HV_{0.1}$			
Average	316.7	331.6	327.5
σ	4.88	5.57	6.81

Table 14.
The average values and standard deviation σ, measuring the share of martensite β'\β$_1$'and its microhardness $HV_{0.1}$ in the microstructure CuAl7Fe5Ni5W2Si2 bronze after annealing τ_ia time

τ_ia, min	30	60	120
Share of martensite, %			
Average	56.6	72.6	49.7
σ	7.78	10.73	11.48
$HV_{0.1}$			
Average	374.6	401.3	366.5
σ	5.31	5.91	9.06

3. Conclusions

From the research of effect of isothermal annealing time, respectively 30, 60 and 120 minutes at 1000°C before quenching CuAl7Fe5Ni5W2Si2 bronze in 10% NaCl solution in water, derive conclusions:

1 - T1 stage - during heating of samples:
- with increasing temperature, dissolved in the β phase matrix sequentially of the phase or phase systems in specific temperature range for which the transformation temperature is lower than 1000°C,
- intermetallic phases such κ_{II} dissolve partially, due to the relatively high rate of heating of the sample and the transformation temperature (> 950°C), slightly lower than 1000°C,
- high tungsten primary intermetallic IM_W phase and primary κ_I phase does not dissolve during heating of samples;

2 - T2 stage - isothermal annealing the samples at 1000°C:
- regardless of annealing time, sample temperature decreases (by about 4°C) due to the fact that energy is absorbed by the following processes:
  - complete the process of dissolving phases κ_{II} in β phase,
  - homogenization of admixtures in β phase,
  - partial transformation of disordered β phase in the β_1 phase ordered,
  - homogenization of admixtures in the primary intermetallic IM_W\κ_I phases,
  - coagulation the primary IM_W\κ_I phases,
  - coalescence the primary IM_W\κ_I phases;

3 - stage T3 and T4 - samples intensive cooling (quenching):
- the microstructure of bronze, on the borders of the secondary β phases α phase is precipitated,
- precipitation of α phase allow size evaluation of the secondary β phase grains,
- lengthening the time of isothermal annealing the tested bronze promotes size reduction β phase,
- after 60 min annealing at 1000°C tested bronze obtained:
  - the highest cooling rate of the sample (-135.6°C/s),
  - the greatest number of hard martensite β'\β_1' (72.6%, 401.3 $HV_{0.1}$)
  - the least amount of bainite α'+β\β1+β'\β_1 ', but characterized by the highest microhardness (11.9%, 331.6 $HV_{0.1}$)
  - the least amount of α phase, precipitated within the secondary β phase (0.2%),
  - the least amount of α phase precipitation, which forms of narrow interphase border of the secondary β phase (1.6%, the average wide precipitation 0.51 μm).

Acknowledgement

The work was conducted in the frames of the research project N N508 399137- financed with the sources for the science in the years 2009-2012 by the Ministry of Science and Higher Education

References

[1] Brezina P. (1973). Gefügeumwandlungen und mechanische Eigenschaften der Mehrstoff-Aluminiumbronzen vom Typ CuAl10 Fe5 Ni5. *Giesserei-Forschung, 25* (3), 1-10.
[2] Süry P., Oswald H.R. (1972). On the corrosion behavior of individual phases present in aluminium bronzes. *Corrosion Science. 12* (1), 77-80. http://dx.doi.org/10.1016/S0010-938X(72)90581-1.
[3] Culpan E.A., Rose G. (1978). Microstructural characterization of cast nickel aluminium bronze. *Journal of Materials Science*, *13* (8), 1647-1657. DOI: 10.1007/BF00548728.
[4] Pisarek B. (2007). The crystallization of the bronze with additions of Si, Cr, Mo and/or W. *Archives of Materials Science and Engineering. 28* (8), 461-466.
[5] Pisarek B. (2007). Influence Cr on crystallization and the phases transformations of the bronze BA1044. *Archives of Foundry Engineering*. *7* (3), 129-136.
[6] Pisarek B. (2008) Abrasive wear of BA1055 bronze with additives of Si, Cr, Mo and/or W. *Archives of Foundry Engineering. 8* (3), 209–216.
[7] Pisarek B. (2008).The influence of wall thickness on the microstructure of bronze BA1055 with the additions of Si, Cr, Mo and/or W. *Archives of Foundry Engineering. 8* (4), 185-192.
[8] Pisarek B. (2010). Influence of the technology of melting and inoculation preliminary alloy AlBe5 on change of concentration of Al and microstructure of the bronze CuAl10Ni5Fe4. *Archives of Foundry Engineering*. *10* (2), 127-134.
[9] Pisarek B. (2011). Effect of additions Cr, Mo, W and/or Si on the technological properties on the technological properties of aluminium-iron-nickel bronze. *Archives of Foundry Engineering*. 1 (3), 199-208.
[10] Erdmann-Jesitzer F., Louis H., Petersen J. (1977). Kavitation von CuAl10 nach thermischer Vorbehandlung. *Metall. 31*, 59-63.
[11] Fortina G., Leoni M. (1973). Compertamento alla corrosione in ambiante marino dei bronzi di alluminio al cobalto. *Metallurgia Italiana. 6*, 363-368.
[12] Górny Z., Sobczak J. (2005). *Nowoczesne tworzywa odlewnicze na bazie metali nieżelaznych*. Kraków: ZA-PIS.
[13] Standnes A. (2007, July). *Thermal Conductivity of Periodic Table Elements*. Retrieved May 7, 2012, From http://www.standnes.no/chemix/periodictable/thermal-conductivity-table.htm
[14] Kirk-Othmer (1999-2011). Copper alloys. Cast copper alloys. *Encyclopedia of Chemical Technology*. John Wiley & Sons, Inc. DOI: 10.1002/0471238961.
[15] Pisarek B. (2011). Effect of two-stage isothermal annealing on microstructure CuAl10Fe5Ni5 bronze with additions of Si, Cr, Mo, W and C. *Archives of Foundry Engineering*. *11*(Spec. Iss.2), 187-194.
[16] Pisarek B. (2011). Simulation of volumetric shrinkage Sv and surface shrinkage Svp. Pietrowski S. (Eds.), *Wysokojakościowe Technologie Odlewnicze, Materiały i Odlewy*, (pp. 167-208), Katowice – Gliwice, PAN.